DESY 01-053
April 2001

Multiplicity moments in deep inelastic scattering at HERA

ZEUS Collaboration

Abstract

Multiplicity moments of charged particles in deep inelastic e^+p scattering have been measured with the ZEUS detector at HERA using an integrated luminosity of 38.4 pb^{-1}. The moments for $Q^2 > 1000$ GeV^2 were studied in the current region of the Breit frame. The evolution of the moments was investigated as a function of restricted regions in polar angle and, for the first time, both in the transverse momentum and in absolute momentum of final-state particles. Analytic perturbative QCD predictions in conjunction with the hypothesis of Local Parton-Hadron Duality (LPHD) reproduce the trends of the moments in polar-angle regions, although some discrepancies are observed. For the moments restricted either in transverse or absolute momentum, the analytic results combined with the LPHD hypothesis show considerable deviations from the measurements. The study indicates a large influence of the hadronisation stage on the multiplicity distributions in the restricted phase-space regions studied here, which is inconsistent with the expectations of the LPHD hypothesis.

The ZEUS Collaboration

S. Chekanov, M. Derrick, D. Krakauer, S. Magill, B. Musgrave, A. Pellegrino, J. Repond, R. Stanek, R. Yoshida
Argonne National Laboratory, Argonne, IL, USA [p]

M.C.K. Mattingly
Andrews University, Berrien Springs, MI, USA

P. Antonioli, G. Bari, M. Basile, L. Bellagamba, D. Boscherini[1], A. Bruni, G. Bruni, G. Cara Romeo, L. Cifarelli[2], F. Cindolo, A. Contin, M. Corradi, S. De Pasquale, P. Giusti, G. Iacobucci, G. Levi, A. Margotti, T. Massam, R. Nania, F. Palmonari, A. Pesci, G. Sartorelli, A. Zichichi
University and INFN Bologna, Bologna, Italy [f]

G. Aghuzumtsyan, I. Brock, S. Goers, H. Hartmann, E. Hilger, P. Irrgang, H.-P. Jakob, A. Kappes[3], U.F. Katz[4], R. Kerger, O. Kind, E. Paul, J. Rautenberg, H. Schnurbusch, A. Stifutkin, J. Tandler, K.C. Voss, A. Weber, H. Wieber
Physikalisches Institut der Universität Bonn, Bonn, Germany [c]

D.S. Bailey[5], N.H. Brook[5], J.E. Cole, B. Foster, G.P. Heath, H.F. Heath, S. Robins, E. Rodrigues[6], J. Scott, R.J. Tapper, M. Wing
H.H. Wills Physics Laboratory, University of Bristol, Bristol, U.K. [o]

M. Capua, A. Mastroberardino, M. Schioppa, G. Susinno
Calabria University, Physics Dept.and INFN, Cosenza, Italy [f]

H.Y. Jeoung, J.Y. Kim, J.H. Lee, I.T. Lim, K.J. Ma, M.Y. Pac[7]
Chonnam National University, Kwangju, Korea [h]

A. Caldwell, M. Helbich, W. Liu, X. Liu, B. Mellado, S. Paganis, S. Sampson, W.B. Schmidke, F. Sciulli
Columbia University, Nevis Labs., Irvington on Hudson, N.Y., USA [q]

J. Chwastowski, A. Eskreys, J. Figiel, K. Klimek[8], K. Olkiewicz, M.B. Przybycień[9], P. Stopa, L. Zawiejski
Inst. of Nuclear Physics, Cracow, Poland [j]

B. Bednarek, K. Jeleń, D. Kisielewska, A.M. Kowal[10], M. Kowal, T. Kowalski, B. Mindur, M. Przybycień, E. Rulikowska-Zarębska, L. Suszycki, D. Szuba
Faculty of Physics and Nuclear Techniques, Academy of Mining and Metallurgy, Cracow, Poland [j]

A. Kotański
Jagellonian Univ., Dept. of Physics, Cracow, Poland

L.A.T. Bauerdick[11], U. Behrens, K. Borras, V. Chiochia, J. Crittenden[12], D. Dannheim, K. Desler, G. Drews, A. Fox-Murphy, U. Fricke, A. Geiser, F. Goebel, P. Göttlicher, R. Graciani, T. Haas, W. Hain, G.F. Hartner, K. Hebbel, S. Hillert, W. Koch[13]†, U. Kötz, H. Kowalski, H. Labes, B. Löhr, R. Mankel, J. Martens, M. Martínez, M. Milite, M. Moritz, D. Notz, M.C. Petrucci, A. Polini, A.A. Savin, U. Schneekloth, F. Selonke, S. Stonjek, G. Wolf, U. Wollmer, J.J. Whitmore[14], R. Wichmann[15], C. Youngman, W. Zeuner
Deutsches Elektronen-Synchrotron DESY, Hamburg, Germany

C. Coldewey, A. Lopez-Duran Viani, A. Meyer, S. Schlenstedt
DESY Zeuthen, Zeuthen, Germany

G. Barbagli, E. Gallo, P. G. Pelfer
University and INFN, Florence, Italy [f]

A. Bamberger, A. Benen, N. Coppola, P. Markun, H. Raach[16], S. Wölfle
Fakultät für Physik der Universität Freiburg i.Br., Freiburg i.Br., Germany [c]

M. Bell, P.J. Bussey, A.T. Doyle, C. Glasman, S.W. Lee[17], A. Lupi, G.J. McCance, D.H. Saxon, I.O. Skillicorn
Dept. of Physics and Astronomy, University of Glasgow, Glasgow, U.K. [o]

B. Bodmann, N. Gendner, U. Holm, H. Salehi, K. Wick, A. Yildirim, A. Ziegler
Hamburg University, I. Institute of Exp. Physics, Hamburg, Germany [c]

T. Carli, A. Garfagnini, I. Gialas[18], E. Lohrmann
Hamburg University, II. Institute of Exp. Physics, Hamburg, Germany [c]

C. Foudas, R. Gonçalo[6], K.R. Long, F. Metlica, D.B. Miller, A.D. Tapper, R. Walker
Imperial College London, High Energy Nuclear Physics Group, London, U.K. [o]

P. Cloth, D. Filges
Forschungszentrum Jülich, Institut für Kernphysik, Jülich, Germany

T. Ishii, M. Kuze, K. Nagano, K. Tokushuku[19], S. Yamada, Y. Yamazaki
Institute of Particle and Nuclear Studies, KEK, Tsukuba, Japan [g]

A.N. Barakbaev, E.G. Boos, N.S. Pokrovskiy, B.O. Zhautykov
Institute of Physics and Technology of Ministry of Education and Science of Kazakhstan, Almaty, Kazakhstan

S.H. Ahn, S.B. Lee, S.K. Park
Korea University, Seoul, Korea [h]

H. Lim[17], D. Son
Kyungpook National University, Taegu, Korea [h]

F. Barreiro, G. García, O. González, L. Labarga, J. del Peso, I. Redondo[20], J. Terrón, M. Vázquez
Univer. Autónoma Madrid, Depto de Física Teórica, Madrid, Spain [n]

M. Barbi, F. Corriveau, S. Padhi, D.G. Stairs
McGill University, Dept. of Physics, Montréal, Québec, Canada [a], [b]

T. Tsurugai
Meiji Gakuin University, Faculty of General Education, Yokohama, Japan

A. Antonov, V. Bashkirov[21], P. Danilov, B.A. Dolgoshein, D. Gladkov, V. Sosnovtsev, S. Suchkov
Moscow Engineering Physics Institute, Moscow, Russia [l]

R.K. Dementiev, P.F. Ermolov, Yu.A. Golubkov, I.I. Katkov, L.A. Khein, N.A. Korotkova, I.A. Korzhavina, V.A. Kuzmin, B.B. Levchenko, O.Yu. Lukina, A.S. Proskuryakov, L.M. Shcheglova, A.N. Solomin, N.N. Vlasov, S.A. Zotkin
Moscow State University, Institute of Nuclear Physics, Moscow, Russia [m]

C. Bokel, M. Botje, J. Engelen, S. Grijpink, E. Koffeman, P. Kooijman, S. Schagen, A. van Sighem, E. Tassi, H. Tiecke, N. Tuning, J.J. Velthuis, J. Vossebeld, L. Wiggers, E. de Wolf
NIKHEF and University of Amsterdam, Amsterdam, Netherlands [i]

N. Brümmer, B. Bylsma, L.S. Durkin, J. Gilmore, C.M. Ginsburg, C.L. Kim, T.Y. Ling
Ohio State University, Physics Department, Columbus, Ohio, USA [p]

S. Boogert, A.M. Cooper-Sarkar, R.C.E. Devenish, J. Ferrando, J. Große-Knetter[22], T. Matsushita, M. Rigby, O. Ruske, M.R. Sutton, R. Walczak
Department of Physics, University of Oxford, Oxford U.K. [o]

A. Bertolin, R. Brugnera, R. Carlin, F. Dal Corso, S. Dusini, S. Limentani, A. Longhin, A. Parenti, M. Posocco, L. Stanco, M. Turcato
Dipartimento di Fisica dell' Università and INFN, Padova, Italy [f]

L. Adamczyk[23], L. Iannotti[23], B.Y. Oh, P.R.B. Saull[23], W.S. Toothacker[13]†
Pennsylvania State University, Dept. of Physics, University Park, PA, USA [q]

Y. Iga
Polytechnic University, Sagamihara, Japan [g]

G. D'Agostini, G. Marini, A. Nigro
Dipartimento di Fisica, Univ. 'La Sapienza' and INFN, Rome, Italy [f]

C. Cormack, J.C. Hart, N.A. McCubbin
Rutherford Appleton Laboratory, Chilton, Didcot, Oxon, U.K. [o]

D. Epperson, C. Heusch, H.F.-W. Sadrozinski, A. Seiden, D.C. Williams
University of California, Santa Cruz, CA, USA [p]

I.H. Park
Seoul National University, Seoul, Korea

N. Pavel
Fachbereich Physik der Universität-Gesamthochschule Siegen, Germany [c]

H. Abramowicz, S. Dagan, A. Gabareen, S. Kananov, A. Kreisel, A. Levy
Raymond and Beverly Sackler Faculty of Exact Sciences, School of Physics, Tel-Aviv University, Tel-Aviv, Israel [e]

T. Abe, T. Fusayasu, T. Kohno, K. Umemori, T. Yamashita
Department of Physics, University of Tokyo, Tokyo, Japan [g]

R. Hamatsu, T. Hirose, M. Inuzuka, S. Kitamura[24], K. Matsuzawa, T. Nishimura
Tokyo Metropolitan University, Dept. of Physics, Tokyo, Japan [g]

M. Arneodo[25], N. Cartiglia, R. Cirio, M. Costa, M.I. Ferrero, S. Maselli, V. Monaco, C. Peroni, M. Ruspa, R. Sacchi, A. Solano, A. Staiano
Università di Torino, Dipartimento di Fisica Sperimentale and INFN, Torino, Italy [f]

D.C. Bailey, C.-P. Fagerstroem, R. Galea, T. Koop, G.M. Levman, J.F. Martin, A. Mirea, A. Sabetfakhri
University of Toronto, Dept. of Physics, Toronto, Ont., Canada [a]

J.M. Butterworth, C. Gwenlan, M.E. Hayes, E.A. Heaphy, T.W. Jones, J.B. Lane, B.J. West
University College London, Physics and Astronomy Dept., London, U.K. [o]

J. Ciborowski[26], R. Ciesielski, G. Grzelak, R.J. Nowak, J.M. Pawlak, P. Plucinski, B. Smalska[27], T. Tymieniecka, J. Ukleja, J.A. Zakrzewski, A.F. Żarnecki
Warsaw University, Institute of Experimental Physics, Warsaw, Poland [j]

M. Adamus, J. Sztuk
Institute for Nuclear Studies, Warsaw, Poland [j]

O. Deppe[28], Y. Eisenberg, L.K. Gladilin[29], D. Hochman, U. Karshon
Weizmann Institute, Department of Particle Physics, Rehovot, Israel [d]

J. Breitweg, D. Chapin, R. Cross, D. Kçira, S. Lammers, D.D. Reeder, W.H. Smith
University of Wisconsin, Dept. of Physics, Madison, WI, USA [p]

A. Deshpande, S. Dhawan, V.W. Hughes P.B. Straub
Yale University, Department of Physics, New Haven, CT, USA [p]

S. Bhadra, C.D. Catterall, W.R. Frisken, R. Hall-Wilton, M. Khakzad, S. Menary
York University, Dept. of Physics, Toronto, Ont., Canada [a]

[1] now visiting scientist at DESY
[2] now at Univ. of Salerno and INFN Napoli, Italy
[3] supported by the GIF, contract I-523-13.7/97
[4] on leave of absence at University of Erlangen-Nürnberg, Germany
[5] PPARC Advanced fellow
[6] supported by the Portuguese Foundation for Science and Technology (FCT)
[7] now at Dongshin University, Naju, Korea
[8] supported by the Polish State Committee for Scientific Research grant no. 5 P-03B 08720
[9] now at Northwestern Univ., Evaston/IL, USA
[10] supported by the Polish State Committee for Scientific Research grant no. 5 P-03B 13720
[11] now at Fermilab, Batavia/IL, USA
[12] on leave of absence from Bonn University
[13] deceased
[14] on leave from Penn State University, USA
[15] partly supported by Penn State University and GIF, contract I-523-013.07/97
[16] supported by DESY
[17] partly supported by an ICSC-World Laboratory Björn H. Wiik Scholarship
[18] visitor of Univ. of the Aegean, Greece
[19] also at University of Tokyo
[20] supported by the Comunidad Autonoma de Madrid
[21] now at Loma Linda University, Loma Linda, CA, USA
[22] now at CERN, Geneva, Switzerland
[23] partly supported by Tel Aviv University
[24] present address: Tokyo Metropolitan University of Health Sciences, Tokyo 116-8551, Japan
[25] now also at Università del Piemonte Orientale, I-28100 Novara, Italy
[26] and Łódź University, Poland
[27] supported by the Polish State Committee for Scientific Research, grant no. 2P03B 002 19
[28] now at EVOTEC BioSystems AG, Hamburg, Germany
[29] on leave from MSU, partly supported by University of Wisconsin via the U.S.-Israel BSF

[a] supported by the Natural Sciences and Engineering Research Council of Canada (NSERC)
[b] supported by the FCAR of Québec, Canada
[c] supported by the German Federal Ministry for Education and Science, Research and Technology (BMBF), under contract numbers 057BN19P, 057FR19P, 057HH19P, 057HH29P, 057SI75I
[d] supported by the MINERVA Gesellschaft für Forschung GmbH, the Israel Science Foundation, the U.S.-Israel Binational Science Foundation, the Israel Ministry of Science and the Benozyio Center for High Energy Physics
[e] supported by the German-Israeli Foundation, the Israel Science Foundation, and by the Israel Ministry of Science
[f] supported by the Italian National Institute for Nuclear Physics (INFN)
[g] supported by the Japanese Ministry of Education, Science and Culture (the Monbusho) and its grants for Scientific Research
[h] supported by the Korean Ministry of Education and Korea Science and Engineering Foundation
[i] supported by the Netherlands Foundation for Research on Matter (FOM)
[j] supported by the Polish State Committee for Scientific Research, grant no. 2P03B04616, 620/E-77/SPUB-M/DESY/P-03/DZ 247/2000 and 112/E-356/SPUB-M/DESY/P-03/DZ 3001/2000
[l] partially supported by the German Federal Ministry for Education and Science, Research and Technology (BMBF)
[m] supported by the Fund for Fundamental Research of Russian Ministry for Science and Education and by the German Federal Ministry for Education and Science, Research and Technology (BMBF)
[n] supported by the Spanish Ministry of Education and Science through funds provided by CICYT
[o] supported by the Particle Physics and Astronomy Research Council, UK
[p] supported by the US Department of Energy
[q] supported by the US National Science Foundation

1 Introduction

The hadronic final state in deep inelastic scattering (DIS) events is the result of a hard partonic scattering initiated at large momentum transfers, $Q \gg \Lambda$, where Λ is a characteristic QCD scale of the order of a few hundred MeV. The subsequent parton cascade is followed by a soft fragmentation process. The latter occurs with small momentum transfers which may be considered to extend up to a value Q_0, which is a QCD cut-off above which perturbative methods can be applied. There are two main approaches for describing the hadronic final state. The first comprises analytic perturbative QCD calculations based on the hypothesis of Local Parton-Hadron Duality (LPHD) [1]; this hypothesis states that parton-level QCD predictions are applicable for sufficiently inclusive hadronic observables, without additional assumptions about hadronisation processes. Therefore, the hadronic spectra are proportional to those of partons if the cut-off Q_0 is decreased towards a small value of Λ. The second approach is formulated in Monte Carlo (MC) programs, which generate a partonic final state according to the perturbative QCD picture and, below $Q_0 \simeq 1$ GeV, hadronise the partons on the basis of non-perturbative models. The MC models are able to reproduce many detailed properties of the hadronic final state, but contain a large number of free parameters.

Multiplicity distributions and correlations between final-state particles are an important testing ground for analytic perturbative QCD in conjunction with the LPHD hypothesis, as well as for MC models describing the hadronic final state [2]. In this paper, a recent analysis of two-particle angular correlations [3] is extended to a study of multiplicity distributions measured in restricted phase-space regions of neutral current DIS events. The particle multiplicities are studied in terms of the normalised factorial moments[1]

$$F_q(\Omega) = \langle n(n-1)\dots(n-q+1)\rangle / \langle n\rangle^q, \qquad q = 2, 3, \dots ,$$

for a specified phase-space region of size Ω. The number, n, of particles is measured inside Ω and angled brackets $\langle \dots \rangle$ denote the average over all events. The factorial moments, along with cumulants [4] and bunching parameters [5], are convenient tools to characterise the multiplicity distributions when Ω becomes small. For uncorrelated particle production within Ω, Poisson statistics holds and $F_q = 1$ for all q. Correlations between particles lead to a broadening of the multiplicity distribution and to dynamical fluctuations. In this case, the normalised factorial moments increase with decreasing Ω. If the rise follows a power law, this effect is frequently called "intermittency" [6].

The LPHD hypothesis, originally suggested for single-particle spectra, presently has experimental support in e^+e^- annihilations [7]. However, the success of LPHD is less evident for the moments of inclusive single-particle densities at HERA energies [8] and two-particle angular correlations [3]. In contrast to the single-particle densities and global event-shape variables, the factorial moments are most directly affected by inclusive *many*-particle densities. This can be seen from the relation $\langle n(n-1)\dots(n-q+1)\rangle = \int_\Omega \rho^{(q)}(p_1, \dots p_q) dp_1 \dots dp_q$ between the factorial moments in a region Ω and the inclusive q-particle density, $\rho^{(q)}(p_1, \dots p_q) = (1/\sigma_{tot})\ d^q\sigma/dp_1 \dots dp_q$. The latter represents the probability to detect q particles with

[1] It may be noted that, for $q = 1$, $F_q = 1$ by definition

momenta $p_1, \ldots p_q$, irrespective of the presence of any other particles. Thus the factorial moments are an important tool to study such densities, for which the applicability of LPHD remains questionable even for higher e^+e^- energies at LEP [9, 10]. Deviations of the measured moments from theoretical predictions would imply the necessity for further refinements of perturbative QCD calculations and/or the failure of the LPHD hypothesis. In the latter case, the magnitude of such deviations can shed light on details of the hadronisation processes.

2 Analytic QCD results

The dominant source of particle production inside a jet is gluon splitting in the QCD cascade, where the presence of a gluon enhances the probability for emission of another gluon nearby in momentum space. This leads to inter-parton correlations and non-Poissonian statistics for the multiplicity distributions in restricted phase-space intervals where partons are counted. Thus the factorial moments, F_q, are expected to deviate from unity.

There exist a number of analytic QCD predictions for the moments of the parton multiplicity distributions obtained in the Double Leading Log Approximation (DLLA), which are discussed below.

2.1 Multiplicity-cut moments

The normalised factorial moments of the multiplicity distributions of gluons which are restricted in either transverse momentum $p_t < p_t^{\rm cut}$ or absolute momentum $p \equiv |\,\mathbf{p}\,| < p^{\rm cut}$ are expected, respectively, to have the following behaviour [11]:

$$\begin{aligned} F_q(p_t^{\rm cut}) &\simeq 1 + \frac{q(q-1)}{6}\,\frac{\ln(p_t^{\rm cut}/Q_0)}{\ln(E/Q_0)}, \\ F_q(p^{\rm cut}) &\simeq C(q) > 1, \end{aligned} \tag{1}$$

where E is the initial energy of the outgoing quark that radiates the gluons and $C(q)$ are constants depending on q. The maximum transverse momentum, $p_t^{\rm cut}$, and the p_t values are defined with respect to the direction of this quark (see Fig. 1(a) for a schematic representation in the case of DIS).

Equations (1) indicate that there are positive correlations between partons, because the factorial moments are larger than unity. For small $p_t^{\rm cut}$ values, however, the correlations vanish due to the presence of an angular ordering of the partons in the jet. The existence of the angular ordering leads to the absence of branching processes with secondary gluon emission at small $p_t^{\rm cut}$. This ultimately leads to the suppression of the correlations in this phase-space region and to independent parton emission[2] ($F_q \simeq 1$ for $p_t^{\rm cut} = Q_0$). On the

[2] Note that this effect is similar to multiple photon bremsstrahlung in QED.

other hand, the distribution of soft gluons with limited absolute momenta, $p < p^{\rm cut}$, remains non-Poissonian for any small value of $p^{\rm cut}$.

Note that the theoretical formulae (1) can be regarded as asymptotic calculations, i.e. they are valid at small $p_t^{\rm cut}$ and $p^{\rm cut}$. Therefore, the calculations should be considered only as qualitative predictions when compared to the data using the LPHD hypothesis.

2.2 Angular moments

Gluon multiplicities in polar-angle rings around the outgoing-quark direction are expected to exhibit a distribution which is substantially wider than for Poisson statistics [12–14]. The moments rise with increasing values of the phase-space variable z as

$$\ln \frac{F_q(z)}{F_q(0)} = z\, a\, (1 - D_q)(q - 1), \tag{2}$$

where z and the constant a are defined as:

$$\begin{aligned} z &= a^{-1} \ln \frac{\Theta_0}{\Theta}, \\ a &= \ln \frac{E\Theta_0}{\Lambda}. \end{aligned} \tag{3}$$

The angle Θ_0 is the half opening-angle of a cone around the outgoing quark radiating the gluons, E is its energy, and Λ is an effective QCD scale ($\Lambda \neq \Lambda_{\overline{MS}}$). A schematic representation of the variables is shown in Fig. 1(b), in which a window in the angular half-width Θ is subtended by the ring centered at Θ_0. The factors D_q are the so-called Rényi dimensions [15] known from non-linear physics. A decrease of the angular window Θ corresponds to an increase of the variable z. The maximum possible phase-space region ($\Theta = \Theta_0$), corresponding to $z = 0$, is used to calculate the factorial moments, $F_q(0)$, which are necessary for normalisation in Eq. (2). Such normalisation removes the theoretical uncertainty in the absolute values of $F_q(z)$ and thus allows a comparison of the predicted z-dependence of the moments with experimental results.

For independent particle production in a restricted range of 2Θ, $D_q = 1$ and $F_q(z) = F_q(0)$ in Eq. (2). In contrast, the analytic QCD expectations for D_q obtained in the DLLA are as follows [12–14]:

- if the strong coupling constant, α_s, is fixed at scale $Q \simeq E\Theta_0$, then for large angular bins (i.e. small z),

$$D_q = \gamma_0 \frac{q+1}{q}, \tag{4}$$

  where $\gamma_0 = \sqrt{2\, C_{\rm A} \alpha_s/\pi}$ is the anomalous QCD dimension, and $C_{\rm A} = 3$ is the gluon colour factor. The α_s value is calculated at the one-loop level with $n_f = 3$ (number

of flavours). Such a behaviour of the moments corresponds to the expectations from intermittency, which can be interpreted in terms of the fractal structure of the gluon splittings [2].

For running-α_s values, the D_q can be approximated by different expressions, depending on the treatment of the non-leading DLLA contributions to the moments:

- for Dokshitzer and Dremin [12]:

$$D_q \simeq \gamma_0 \frac{q+1}{q}\left(1+\frac{q^2+1}{4q^2}z\right); \tag{5}$$

- for Brax et al. [13]:

$$D_q \simeq 2\,\gamma_0 \frac{q+1}{q}\left(\frac{1-\sqrt{1-z}}{z}\right); \tag{6}$$

- for Ochs and Wosiek [14]:

$$D_q \simeq 2\,\gamma_0 \frac{q-w(q,z)}{z(q-1)}, \qquad w(q,z) = q\sqrt{1-z}\left(1-\frac{\ln(1-z)}{2q^2}\right); \tag{7}$$

- an estimate for D_q which includes a correction from the Modified Leading Log Approximation (MLLA) has also been obtained by Dokshitzer and Dremin [12]. In this case, Eq. (5) remains valid, but γ_0 is replaced by an effective $\gamma_0^{\rm eff}(q)$ which depends on q.

All the theoretical calculations quoted above are performed for partons. Therefore, for comparisons of the predictions with data, LPHD is assumed.

3 Experimental set-up

The data were taken in 1996 and 1997 using the ZEUS detector at HERA. During this period, the energy of the positron beam, E_e, was 27.5 GeV and that of the proton beam was 820 GeV. The integrated luminosity used for the present study was 38.4 ± 0.6 pb^{-1}.

ZEUS is a multi-purpose detector described in detail elsewhere [16]. Of particular importance for the present study are the central tracking detector (CTD), positioned in a 1.43 T solenoidal magnetic field, and the calorimeter.

The CTD is a cylindrical drift chamber with nine superlayers covering the polar angle[3] region $15^o < \theta \leq 164^o$ and the radial range 18.2-79.4 cm. Each superlayer consists of eight

[3] The ZEUS coordinate system is a right-handed Cartesian system, with the Z axis pointing in the proton beam direction, and the X axis pointing left towards the centre of HERA. The coordinate origin is at the nominal interaction point. The polar angle θ is defined with respect to the positive Z-direction. The pseudorapidity, η, is given by $-\ln(\tan\frac{\theta}{2})$.

anodes. The transverse-momentum resolution for charged tracks traversing all CTD layers is $\sigma(p_\perp)/p_\perp = 0.0058p_\perp \oplus 0.0065 \oplus 0.0014/p_\perp$, with $p_\perp$ being the track-transverse momentum (in GeV). The single hit efficiency of the CTD is greater than 95%.

The CTD is surrounded by the uranium-scintillator calorimeter (CAL), which is longitudinally segmented into electromagnetic and hadronic sections. The relative energy resolution of the calorimeter under test beam conditions is $0.18/\sqrt{E}$ for electrons and $0.35/\sqrt{E}$ for hadrons (with E in GeV). The CAL cells provide time measurements with a time resolution below 1 ns for energy deposits larger than 4.5 GeV.

4 Data selection

4.1 Event kinematics

The basic event kinematics of DIS processes are determined by the negative squared four-momentum transfer at the positron vertex, $Q^2 = -q^2 = -(k - k')^2$ (k and k' denote the four-momenta of the initial- and final-state positrons, respectively) and the Bjorken scaling variable $x = Q^2/(2P \cdot q)$, where P is the four-momentum of the proton. The fraction of the energy transfered to the proton in its rest frame, y, is related to these two variables by $y \simeq Q^2/sx$, where $\sqrt{s}$ is the positron-proton centre-of-mass energy.

The moments were studied in the Breit frame [17], which provides a natural system to separate the radiation from the outgoing struck quark from the proton remnants. In this frame, the exchanged virtual boson with virtuality Q^2 is completely space-like and has a momentum $q = (q_0, q_{X_\mathrm{B}}, q_{Y_\mathrm{B}}, q_{Z_\mathrm{B}}) = (0, 0, 0, -Q)$. In the quark-parton model, the incident quark has $p_{Z_\mathrm{B}} = Q/2$ and the outgoing struck quark carries $p_{Z_\mathrm{B}} = -Q/2$. All particles with negative p_{Z_B} form the current region. These particles are produced by the fragmentation of the struck quark, so that the current region is analogous to a single hemisphere in e^+e^- annihilations. The variables $p_t = \sqrt{p_{X_\mathrm{B}}^2 + p_{Y_\mathrm{B}}^2}$ and Θ_0 were determined with respect to the negative Z_B-direction, which, for high Q^2 events, is a good estimate of the outgoing struck-quark direction. The moments in the current region of the Breit frame were measured in the kinematic region $Q^2 > 1000$ GeV^2, which is sufficiently high to avoid major contributions from the boson-gluon fusion (BGF) processes (see Section 7).

4.2 Event and track selection

The kinematic variables x and Q^2 were determined by a combination of methods: (i) the measurement of the energy and angle of the scattered positron (denoted by the subscript e); (ii) the double angle (DA) method [18] and (iii) the Jacquet-Blondel (JB) method [19], depending on which is most appropriate for a particular cut. In the DA method, the variables x, Q^2 and y were reconstructed using the angles of the scattered positron and the hadronic energy flow. In the JB method, used only in the event selection, the kinematic variables were determined entirely from the hadronic system.

The boost vector from the laboratory to the Breit frame was determined using the DA method, which is less sensitive to systematic uncertainties in the energy measurement than the other methods. In the reconstruction of the Breit frame, all charged particles were assumed to have the pion mass.

The triggering and online event selections were identical to those used in a previous publication [20]. To preselect neutral current DIS events, the following cuts were applied:

- $E_e^{'} \geq 10$ GeV, $E_e^{'}$ being the energy of the scattered positron;
- $Q^2_{\rm DA} \geq 1000$ GeV^2;
- $35 \leq \delta = \sum E_i(1-\cos\theta_i) \leq 60$ GeV, where E_i is the energy of the $i^{\rm th}$ calorimeter cell and θ_i is its polar angle with respect to the beam axis;
- $y_e \leq 0.95$;
- $y_{\rm JB} \geq 0.04$;
- Z coordinate of the reconstructed vertex position, as determined from the tracks fitted to the vertex, in the range $-40 < Z_{\rm vertex} < 50$ cm;
- a timing cut requiring that the event time as measured by the CAL be consistent with an e^+p interaction.

The resulting data set contained 7369 events.

The present study is based on the tracks reconstructed with the CTD and fitted to the event vertex. The scattered positron was removed from the track sample. In addition, the following cuts to select tracks were imposed:

- $p_t^{lab} > 0.15$ GeV, where p_t^{lab} is the transverse momentum of the track;
- $|\,\eta\,| < 1.75$.

These cuts restrict the data to a well understood, high-acceptance region of the CTD.

5 Event simulation

Neutral current DIS events were generated with ARIADNE 4.10 [21] with the high Q^2 modification developed during the HERA Monte Carlo workshop [22] using tuned parameters [23]. This MC program is based on the colour-dipole model, in which gluons are emitted from the colour field between quark-antiquark pairs, supplemented with the BGF process. The hadronisation was simulated using the Lund string model as implemented in JETSET [24].

Charged hadrons with a mean lifetime longer than 10^{-8} seconds were considered as stable. The CTEQ4D [25] parameterisation of the proton parton distribution functions was used. The events were generated without any cuts on kinematic variables and track quantities. The MC events obtained by this procedure defined the generator-level sample.

To obtain a detector-level sample, events were generated with the DJANGO 6.24 [26] program based on HERACLES 4.5.2 [27], in order to incorporate first-order electroweak corrections. The parton cascade and hadronisation were then simulated with ARIADNE. The events were then processed through a simulation of the detector using GEANT 3.13 [28] to take into account particle interactions with the detector material, particle decays, event and track migrations, resolution, acceptance of the detector and event selection. The detector-level MC events were processed with the same reconstruction program as was used for the data.

In addition to ARIADNE, the LEPTO 6.5 [29] and HERWIG 5.9 [30] generators with tuned parameters [23] were also used to compare with the data. The parton cascade in LEPTO is based on a matrix-element calculation matched to parton showers according to the DGLAP equations. As in ARIADNE, the hadronisation in LEPTO is simulated with JETSET. HERWIG also has a parton shower based on DGLAP evolution, but parton emissions are ordered in angle, in contrast to LEPTO, which orders the parton emissions in invariant mass with an additional angular constraint to ensure coherence. The hadronisation in HERWIG is described by the cluster fragmentation model [31].

The Bose-Einstein (BE) interference between identical particles can produce additional correlations which distort the behaviour of the moments measured in small phase-space regions. By default, the BE interference is turned off in JETSET; it is absent in HERWIG. The effect of the BE correlations on the present results is considered in the next section.

6 Correction procedure

The bin-by-bin correction factors, $\mathcal{C}_q = \mathcal{A}_q^{\rm gen}/\mathcal{A}_q^{\rm det}$, for a given kinematic region in Q^2 were evaluated using the ARIADNE 4.10 MC event samples, separately for each observable, $\mathcal{A}_q = F_q(p_t^{\rm cut}), F_q(p^{\rm cut})$ and $F_q(z)/F_q(0)$, where $\mathcal{A}_q^{\rm gen}$ ($\mathcal{A}_q^{\rm det}$) was calculated at the generator (detector) level. The factors $\mathcal{C}_q$ correct the data for the detector effects and event-selection cuts as well as for the effects that are not included in the analytic calculations, namely (i) Dalitz decays of the π^0; (ii) leptons in the final state and (iii) initial-state photon radiation.

The correction factors for the $p_t^{\rm cut}$ and $p^{\rm cut}$ moments are approximately flat and vary between about 1.0 and 1.3, except for the smallest momentum cuts and the highest-order $p_t^{\rm cut}$ and $p^{\rm cut}$ moments, where the correction factors are as large as 1.7. The correction factors for the $F_q(z)/F_q(0)$ moments vary smoothly from 1.0 to 1.5. The contribution of Dalitz pairs to the correction factors is negligible, except for the smallest phase-space regions in $p_t^{\rm cut}$, $p^{\rm cut}$ and Θ, where it does not exceed 20%.

The analytic QCD calculations do not include BE interference. To take into account this

phenomenon, the correction factor, BE_q, was calculated for each data point

$$\mathrm{BE}_q = \frac{\mathcal{A}_q^{\mathrm{gen}}}{\mathcal{A}_q^{\mathrm{BE,\,gen}}} \ , \tag{8}$$

where $\mathcal{A}_q^{\mathrm{gen}}$ ($\mathcal{A}_q^{\mathrm{BE,\,gen}}$) are the moments at the generator level without (with) the BE effect. For this correction, the BE effect according to a Gaussian parameterisation with JETSET default parameters was used. As a cross check, the BE correction was determined from the ZEUS data and also using the parameters obtained by the H1 Collaboration [32]. The differences between the correction factors BE_q for these three sets of parameters were small. The values of the BE correction factors are discussed in Section 8.

7 Systematic uncertainties

The overall systematic uncertainty for each moment was determined from the following uncertainties added in quadrature:

- the choice of the MC models. HERWIG was used in place of ARIADNE to determine the correction factors. This uncertainty was typically 45% of the total systematic uncertainty;
- event reconstruction and selection. Systematic checks were performed by varying the cuts on δ, y_e, y_{JB} and the vertex position requirement ($40 \leq \delta \leq 55$ GeV, $y_e \leq 0.85$, $y_{\mathrm{JB}} \geq 0.05$ and $-35 < Z_{\mathrm{vertex}} < 45$ cm). The overall uncertainties associated with the event selection were typically 25% of the total systematic uncertainty;
- track reconstruction and selection. Tracks were required to have transverse momenta larger than 0.2 GeV and $\mid \eta \mid < 1.5$. Tracks that reach at least the third CTD superlayer were used. These uncertainties were typically 30% of the total systematic uncertainty.

As an example, the total systematic uncertainty of $F_2(p_t^{\mathrm{cut}})$ for the smallest p_t^{cut} value used in this analysis is approximately 6%. For the large p_t^{cut} regions, a typical value of the systematic uncertainty is 1%.

To ensure that the two particles in a pair were resolved, the angle between two tracks in the current region of the Breit frame should not be smaller than two degrees [3]. This limit determines the minimum size of phase-space regions used in this analysis.

The kinematic variables p_t, Θ and Θ_0 have to be measured with respect to the outgoing-quark direction, which coincides with the Z_{B}-direction of the Breit frame only for the zeroth-order $\gamma^* q$ scattering. The first-order QCD effects, BGF ($\gamma^* g \rightarrow q\overline{q}$) and QCD Compton ($\gamma^* q \rightarrow qg$), can lead to two hard partons that are not collinear to the Z_{B}-direction. For these events, the determination of the kinematic variables with respect to the Z_{B} axis of the Breit frame is inappropriate, especially when these two hard partons escape the current

region. Using the LEPTO MC model, it has been determined that, at $Q^2 > 1000$ GeV^2, the number of BGF and QCD Compton events without hard partons in the current region, relative to the total number of events, is $\leq 15\%$. As a systematic check, the factorial moments have been calculated in kinematic variables with respect to the thrust axis determined from the charged particles in the current region of the Breit frame. The results agree with those for which the negative $Z_{\rm B}$-direction of the Breit frame is used.

8 Results

The charged-particle multiplicities measured in the entire current region without additional momentum cuts on the charged particles were compared to the previous ZEUS measurements [8] and to e^+e^- data [33]. For the present measurement, the corrected average value of Q^2 is $\langle Q^2 \rangle \simeq 2070$ GeV^2, which corresponds to an energy $\sqrt{\langle Q^2 \rangle} \simeq 46$ GeV. The corrected average charged-particle multiplicity in the current region, 5.76 ± 0.29, where the error represents statistical and systematic uncertainties added in quadrature, agrees with the previous ZEUS measurement, 6.01 ± 0.46, for a similar value of $\langle Q^2 \rangle$. This average multiplicity is lower than that found in a single hemisphere of e^+e^- at $\sqrt{s} = 44$ GeV, which is 7.58 ± 0.37 [33]. The second-order factorial moment F_2 in a single hemisphere of e^+e^- annihilations is[4] $F_2 = 1.036 \pm 0.026$, which is consistent with the value 1.051 ± 0.018 obtained in this study of the entire current region. This difference in the average multiplicity can be attributed to a migration of particles between the current and target regions due to BGF and QCD Compton processes, an effect which has been theoretically quantified [34] and directly measured by ZEUS [3]. Such a migration leads to current-target anti-correlations which do not vanish even at the high Q^2 values studied here. This is unlike the e^+e^- annihilation processes, where weak and positive forward-backward correlations have been observed at a similar energy [33].

8.1 Multiplicity-cut moments

The multiplicity moments of order $q = 2, \ldots, 5$ as a function of $p_t^{\rm cut}$ are shown in Fig. 2. The $p_t^{\rm cut}$ moments were calculated with respect to the negative $Z_{\rm B}$-direction of the Breit frame. As $p_t^{\rm cut}$ decreases below 1 GeV, the moments rise. This disagrees with the DLLA theoretical calculations, which predict that the moments approach unity (see Eq. (1)). On the other hand, Monte Carlo models show the same trend as the data, although some differences in slopes are apparent. LEPTO exhibits smaller values of the moments than for the data at small $p_t^{\rm cut}$ values, while HERWIG overestimates the moments. ARIADNE gives the best overall description of the correlations.

Figure 2 also shows the factors BE_q from Eq. (8) used to correct the data for the BE interference. The largest correction was found in the case of moments of high orders ($q = 4, 5$) for small $p_t^{\rm cut}$ cuts (< 0.5 GeV).

[4] The second-order moment in a single hemisphere of e^+e^- annihilation can be estimated from the dispersion $D = \sqrt{\langle n^2 \rangle - \langle n \rangle^2}$ and the average multiplicity $\langle n \rangle$ [33] using the relation $F_2 = 1 + D^2 \langle n \rangle^{-2} - \langle n \rangle^{-1}$.

To investigate contributions of the hadronisation processes to the moments, further samples of the ARIADNE MC were generated: (1) considering neutral hadrons in addition to charged particles; (2) using only hadrons coming from the Lund string fragmentation without resonance decays. For these two cases, the moments have an even steeper rise at low $p_t^{\rm cut}$. Replacing the Lund string-fragmentation scheme by independent fragmentation and removing resonance decays led to an increase of the moments for $p_t^{\rm cut} \simeq 0.5$ GeV, but below this cut the moments approach constant values which are larger than unity. An MC sample generated without the colour-dipole parton emission and resonance decays, but retaining the Lund string fragmentation, leads to an increase of the moments with decreasing $p_t^{\rm cut}$.

Figure 3 shows the factorial moments for restricted p values. As was the case for the $p_t^{\rm cut}$ moments, there is no indication that the values approach unity at small $p^{\rm cut}$ values. All MC models at the hadron level agree with the data. The BE interference has a large influence on this measurement, giving a 20% correction.

The DLLA QCD calculations neglect energy-momentum conservation in gluon splittings, considering idealised jets at asymptotically large energy. This effect can be taken into account in the Modified Leading Log Approximation; however, such calculations have not yet been performed. Therefore, it is important to compare the experimental results with the parton shower of MC models that explicitly include energy-momentum conservation and the complete parton-splitting functions. In addition, such comparisons allow the investigation of the contributions from hadronisation.

The moments restricted in p_t and p variables were determined from the ARIADNE parton-level, the physics implementation of which strongly resembles the analytic calculations [11]. The LPHD requires Q_0 to approach Λ. The ARIADNE default value of Λ is 0.22 GeV, while the transverse momentum cut-off Q_0 is 0.6 GeV. Therefore, to satisfy the LPHD requirement, the parton predictions were obtained after switching off the string fragmentation and lowering the Q_0 value in ARIADNE to $Q_0 = 0.27$ GeV. This value was chosen in order to insure that the average multiplicity of partons in the current region of the Breit frame equalled that of hadrons, which is important for normalisation purposes. This method is somewhat different to that used in a similar study of the ARIADNE parton cascade for e^+e^- annihilation events [11]. In contrast to that approach, the present modification of the model retains the original default value of Λ, to preserve the kinematics of first-order QCD processes in the Breit frame.

The parton-level ARIADNE for $p_t^{\rm cut}$ and $p^{\rm cut}$ moments is shown as thin solid lines in Figs. 2 and 3. Agreement between the parton-level predictions and the data for the lowest $p_t^{\rm cut}$ values can be excluded at greater than 99% confidence level for $q = 2, 3$ and at greater than 95% confidence level for $q = 4, 5$. The data for all $p^{\rm cut}$ moments disagrees with the parton-level predictions by many standard deviations. The MC predictions for partons have the trends expected from the analytic DLLA results, showing a decrease of the moments for decreasing $p_t^{\rm cut}$ and $p^{\rm cut}$. This is contrary both to the measurements and to the hadron-level MC predictions, which show a rise of the moments. Analogous differences between the hadron and parton levels of ARIADNE have also been observed in e^+e^- annihilation [11].

The parton predictions in the full current region (large $p_t^{\rm cut}$ and $p^{\rm cut}$) show larger values of

the moments than the data, despite the tuning of the parton to the hadron multiplicities. In the case of e^+e^-, the MC-tuned parton level describes the hadron-level predictions for large momentum cuts [11]. It is likely that the discrepancy between partons and hadrons in DIS is due to additional non-perturbative effects related to the proton remnant.

8.2 Angular moments

Figure 4 shows the angular moments $F_q(z)/F_q(0)$. This represents the first measurement of these quantities in DIS. The measurements are compared to DLLA QCD calculations in Eq. (2), after substitution of different forms of the Rényi dimension (see Eqs. (4)-(7)) and using the effective QCD parameter $\Lambda = 0.15$ GeV as in LEP studies [9, 10]. For DIS in the Breit frame, the energy $E = Q/2$ was chosen to define the α_s value, corresponding to the outgoing quark momentum in the quark-parton model. The factors used to correct the data for the BE interference are close to unity for all angular moments (not shown). A significant disagreement with the data is observed, which becomes smaller for higher orders of the moments. Although the error bars are clearly correlated, even for the high-order moments, agreement between the predictions and the data can be excluded for z =0.05-0.2 at greater than 95% confidence level. For running-α_s calculations, the best description is observed for high-order moments in the case of the DLLA result with a correction from the MLLA. This result is similar to that obtained for e^+e^- annihilation [9, 10]. It should be noted that the present analysis, however, uses a larger angle $\Theta_0 = 45^o$, in order to increase the statistics, and that the average energy ($\langle E \rangle \simeq 23$ GeV) of the outgoing quark giving rise to the parton shower is smaller than at LEP by a factor of two.

Figure 5 shows the comparisons of the angular moments with Monte Carlo models at the hadron level. All models reproduce the trends of the data but somewhat overestimate the strength of the correlations; however, LEPTO fails to give a reasonable description of the angular moments.

The parton-level ARIADNE predictions for the angular moments are shown in Fig. 5. The ratio $F_q(z)/F_q(0)$ predicted by ARIADNE at the parton level (thin lines) overestimates the data, but is closer than the analytic DLLA calculations for the second-order moment. This comparison with the MC parton level and similar studies of e^+e^- annihilations at LEP [9,10] imply that MLLA analytic calculations are necessary to give a better description of the measured angular moments.

9 Conclusions

Multiplicity moments have been studied in deep inelastic scattering at $Q^2 > 1000$ GeV^2 with the ZEUS detector at HERA. The moments measured in the current region of the Breit frame show a strong rise as the size of the restricted intervals in p_t, p and Θ decreases. Monte Carlo models, which include hadronisation effects, reproduce the correlation pattern of the hadronic final state, although there are some discrepancies with the data.

The analytic QCD calculations for the angular moments agree qualitatively with the data, but there are discrepancies at the quantitative level. An inadequate treatment of energy-momentum conservation in gluon splittings, which is important at low energies, is likely to be responsible for the discrepancies between the analytic QCD expectations and the data. The parton level of ARIADNE, which does not suffer from the limitations of the DLLA calculations, indicates that the discrepancies can be reduced. MLLA calculations are required to provide an accurate description of the angular moments. Similar studies of the angular moments measured at LEP also show that the analytic perturbative calculations need to be improved.

In contrast to the angular fluctuations, the moments calculated in restricted p_t and p regions show significant discrepancies, both for the DLLA calculations and for the parton-level of ARIADNE. This is most clearly seen for the $p_t^{\rm cut}$ moments; while the analytic calculations and ARIADNE predictions for partons decrease and approach unity for small p_t regions, the data show a steep rise. This is the first indication that perturbative QCD, in conjunction with the LPHD hypothesis, fails on a qualitative level to describe the hadronic multiplicities. Monte Carlo studies of the hadronisation effects indicate that this is due to violation of the LPHD hypothesis for many-particle densities measured in the regions restricted in the transverse momenta with respect to the direction of the outgoing quark.

Acknowledgements

The strong support and encouragement of the DESY Directorate have been invaluable, and we are much indebted to the HERA machine group for their inventiveness and diligent efforts. The design, construction and installation of the ZEUS detector have been made possible by the ingenuity and dedicated efforts of many people from inside DESY and from the home institutes who are not listed as authors. Their contributions are acknowledged with great appreciation. We thank W. Ochs and J. Wosiek for helpful discussions.

References

[1] Ya.I. Azimov et al., Z. Phys. C 27 (1985) 65; Z. Phys. C 31 (1986) 213.

[2] E.A. De Wolf, I.M. Dremin and W. Kittel, Phys. Rep. 270 (1996) 1.

[3] ZEUS Collaboration, J. Breitweg et al., Eur. Phys. J C 12 (2000) 53.

[4] A.H. Mueller, Phys. Rev. D 4 (1971) 150.

[5] S.V. Chekanov and V.I. Kuvshinov, Acta Phys. Pol. B 25 (1994) 1189;
S.V. Chekanov, W. Kittel and V.I. Kuvshinov, Z. Phys. C 74 (1997) 517.

[6] A. Białas and R. Peschanski, Nucl. Phys. B 273 (1986) 703; Nucl. Phys. B 308 (1988) 857.

[7] V. A. Khoze and W. Ochs, Int. J. Mod. Phys. A 12 (1997) 2949.

[8] ZEUS Collaboration, J. Breitweg et al., Eur. Phys. J. C 11 (1999) 251.

[9] L3 Collaboration, M. Acciarri et al., Phys. Lett. B 428 (1998) 186;
L3 Collaboration, M. Acciarri et al., Phys. Lett. B 429 (1998) 375.

[10] DELPHI Collaboration, P. Abreu et al., Phys. Lett. B 457 (1999) 368.

[11] S. Lupia, W. Ochs and J. Wosiek, Nucl. Phys. B 540 (1999) 405.

[12] Yu.L. Dokshitzer and I.M. Dremin, Nucl. Phys. B 402 (1993) 139.

[13] P. Brax, J.-L. Meunier and R. Peschanski, Z. Phys. C 62 (1994) 649.

[14] W. Ochs and J. Wosiek, Phys. Lett. B 289 (1992) 159; Phys. Lett. B 305 (1993) 144; Z. Phys. C 68 (1995) 269.

[15] A. Rényi, *Probability Theory*, North-Holland, Amsterdam, (1970);
H.G.E. Hentschel and I. Procaccia, Physica D 8 (1983) 435;
P. Grassberger, Phys. Lett. A 97 (1983) 227.

[16] ZEUS Collaboration, U. Holm (ed.), *The ZEUS Detector*, Status Report, (unpublished), DESY, 1993,
`http://www-zeus.desy.de/bluebook/bluebook.html`.

[17] R. P. Feynman, *Photon-Hadron Interactions*, Benjamin, New York, (1972).

[18] S. Bentvelsen, J. Engelen and P. Kooijman, *Proceedings of the 1991 Workshop on Physics at HERA*, DESY, W. Buchmüller and G. Ingelman (eds.), (1992) p. 23.
K. C. Hoeger, *ibid.*, p.43.

[19] F. Jacquet and A. Blondel, *Proceedings of the study for an ep facility for Europe*, U. Amaldi (ed.), DESY 79-48 (1979) p. 391.

[20] ZEUS Collaboration, M. Derrick et al., Z. Phys. C 72 (1996) 399.

[21] ARIADNE 4.10, L. Lönnblad, Comp. Phys. Comm. 71 (1992) 15.

[22] L. Lönnblad, *Proceedings of the 1998/1999 Workshop on Monte Carlo Generators for HERA Physics*, DESY-PROC-1999-02, A.T. Doyle et al. (eds.), p. 47, `http://www.desy.de/~heramc`.

[23] N. Brook et al., *Proceedings of the 1995/1996 Workshop on Future Physics at HERA*, DESY, G. Ingelman et al. (eds.), (1996) p. 613.

[24] PYTHIA 5.7 and JETSET 7.4, T. Sjöstrand, Comp. Phys. Comm. 82 (1994) 74.

[25] H.L. Lai et al., Phys. Rev. D 51 (1995) 4763;
H.L. Lai et al., Phys. Rev. D 55 (1997) 1280.

[26] DJANGO 6.24, K. Charchuła, G.A. Schuler and H. Spiesberger, Comp. Phys. Comm. 81 (1994) 381.

[27] HERACLES 4.5.2, A. Kwiatkowski, H. Spiesberger and H.-J. Möhring, Comp. Phys. Comm. 69 (1992) 155.

[28] GEANT3, R. Brun et al., CERN-DD/EE/84-1 (1987).

[29] LEPTO 6.5, G. Ingelman, A. Edin and J. Rathsman, Comp. Phys. Comm. 101 (1997) 108.

[30] HERWIG 5.1, G. Marchesini et al., Comp. Phys. Comm. 67 (1992) 465.

[31] G. Marchesini and B.R. Webber, Nucl. Phys. B 310 (1988) 461.

[32] H1 Collaboration, C. Adloff et al., Z. Phys. C 75 (1997) 437.

[33] TASSO Collaboration, W. Braunschweig et al., Z. Phys. C 45 (1989) 193.

[34] S.V. Chekanov, J. Phys. G 25 (1999) 59.

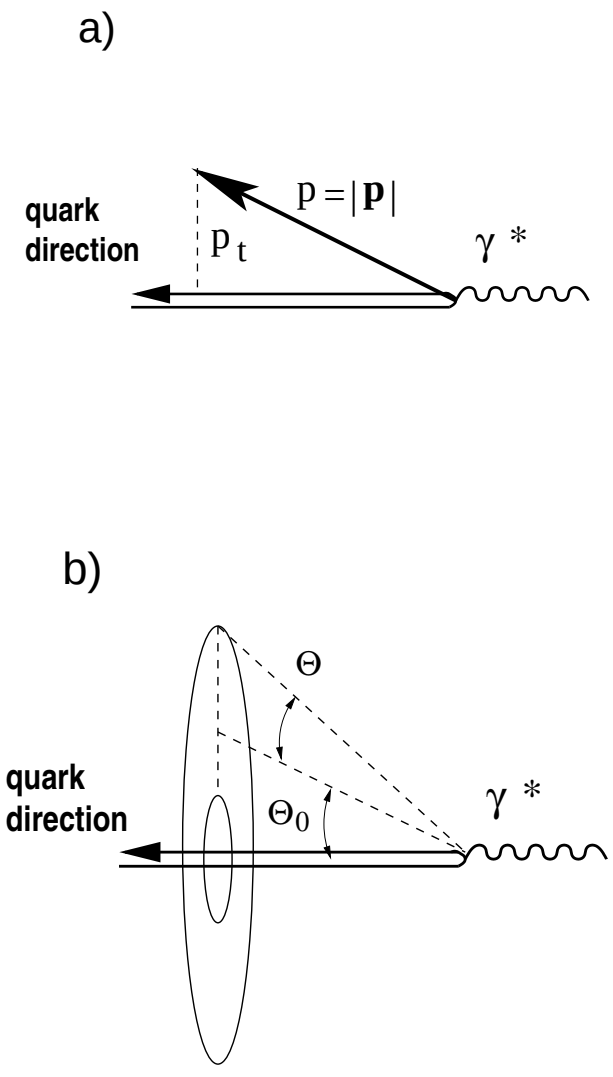

Figure 1: A schematic representation of the measurements of the factorial moments in DIS: (a) restricted in the transverse momentum, p_t, defined with respect to the outgoing-quark direction and absolute momentum, $|\ \mathbf{p}\ |$; (b) in polar-angle rings of width 2Θ.

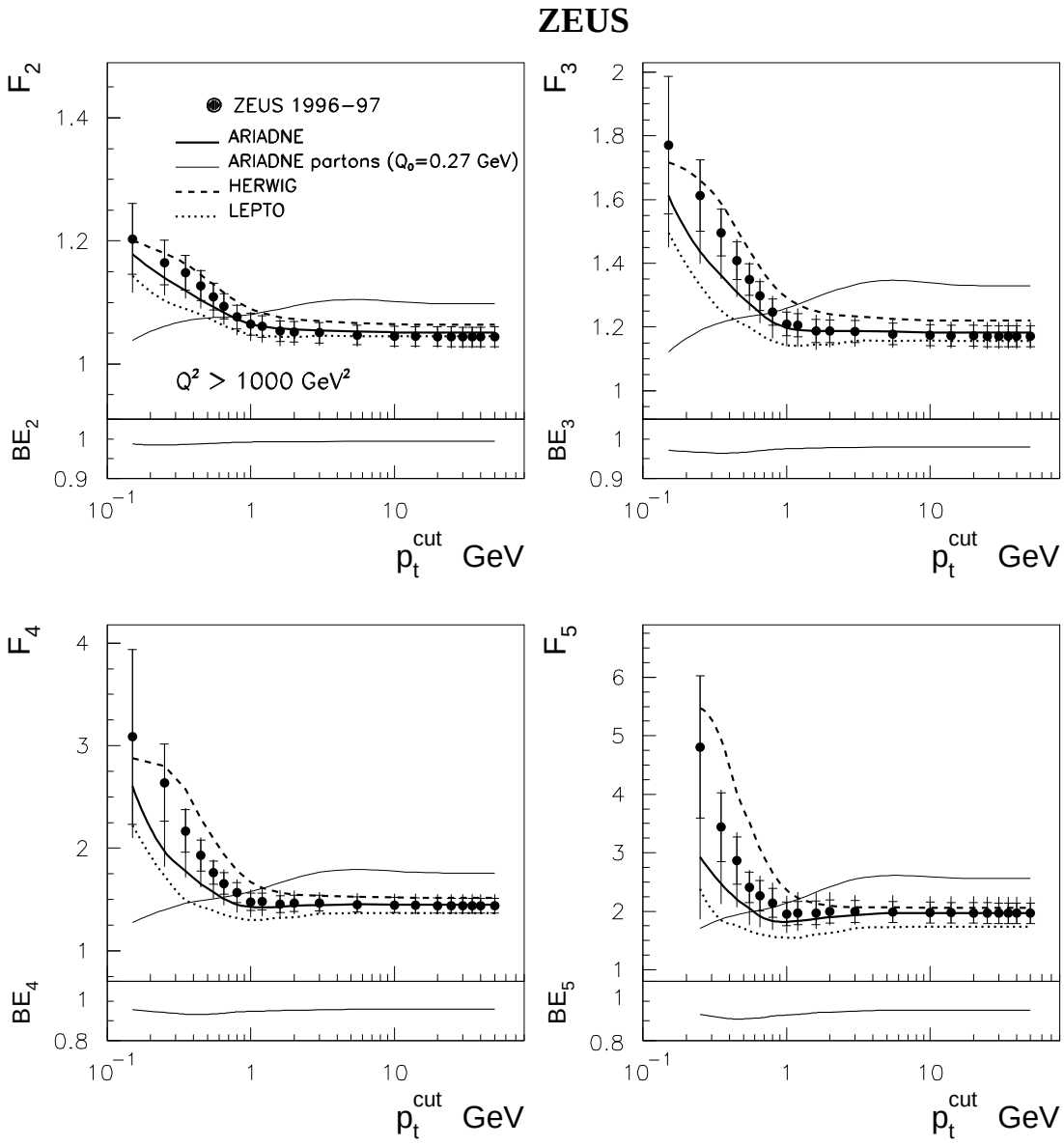

Figure 2: Factorial moments for charged particles in the current region of the Breit frame as a function of $p_t^{\rm cut}$, compared to Monte Carlo models. The thin lines show the parton-level prediction of ARIADNE with $Q_0 = 0.27$ GeV and the thick solid lines are the hadron-level predictions of the same model. The dashed and dotted lines show the hadron-level predictions of HERWIG and LEPTO, respectively. The inner error bars are statistical uncertainties; the outer are statistical and systematic uncertainties added in quadrature. The correction factors for the BE effect are shown below each plot.

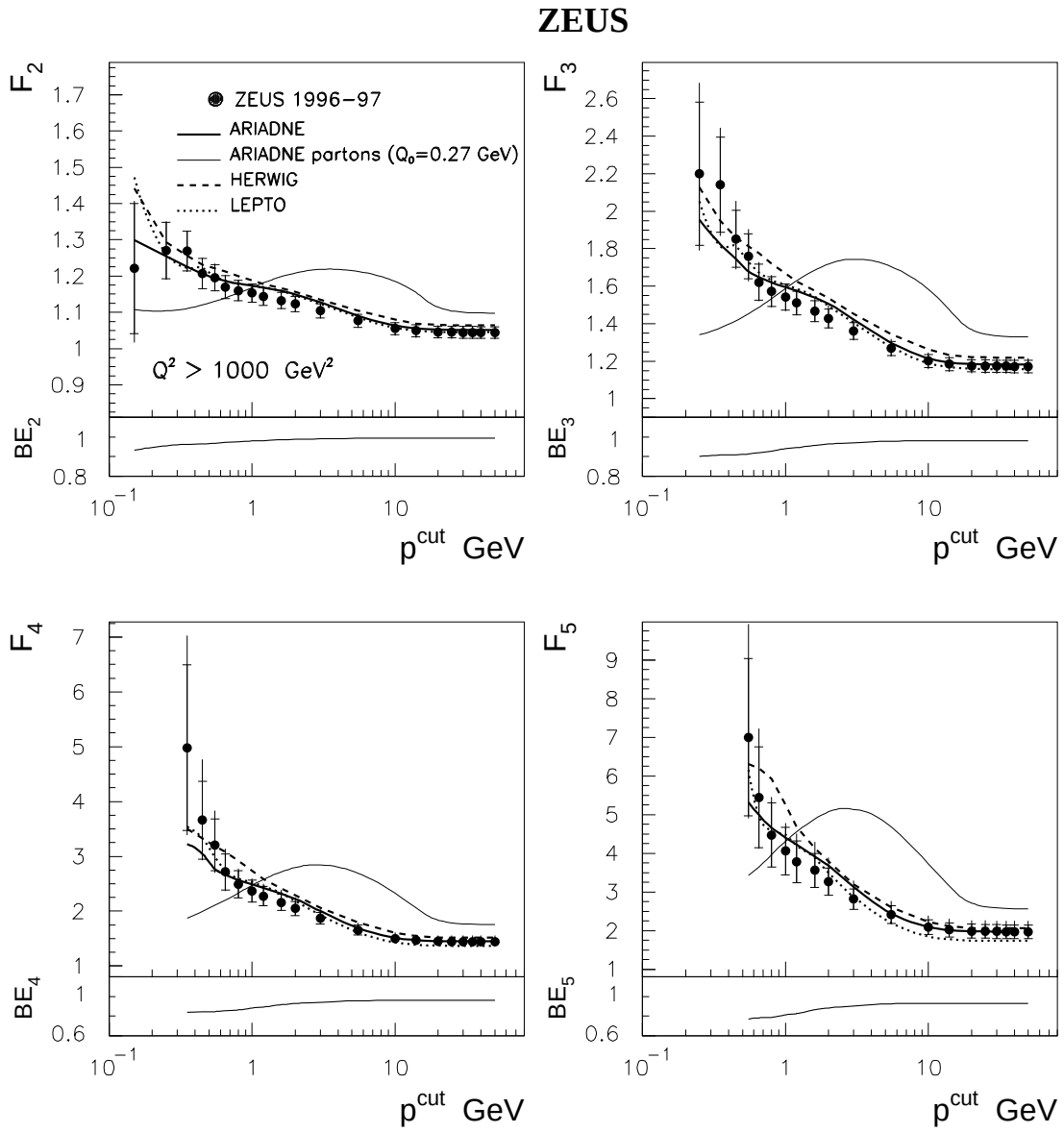

Figure 3: Factorial moments for charged particles in the current region of the Breit frame as a function of $p^{\rm cut}$, compared to Monte Carlo models. The thin solid lines show the parton-level prediction of ARIADNE and the thick solid lines are the hadron-level predictions of the same model. The dashed and dotted lines show the hadron-level predictions of HERWIG and LEPTO, respectively. The inner error bars are statistical uncertainties; the outer are statistical and systematic uncertainties added in quadrature. The correction factors for the BE effect are shown below each plot.

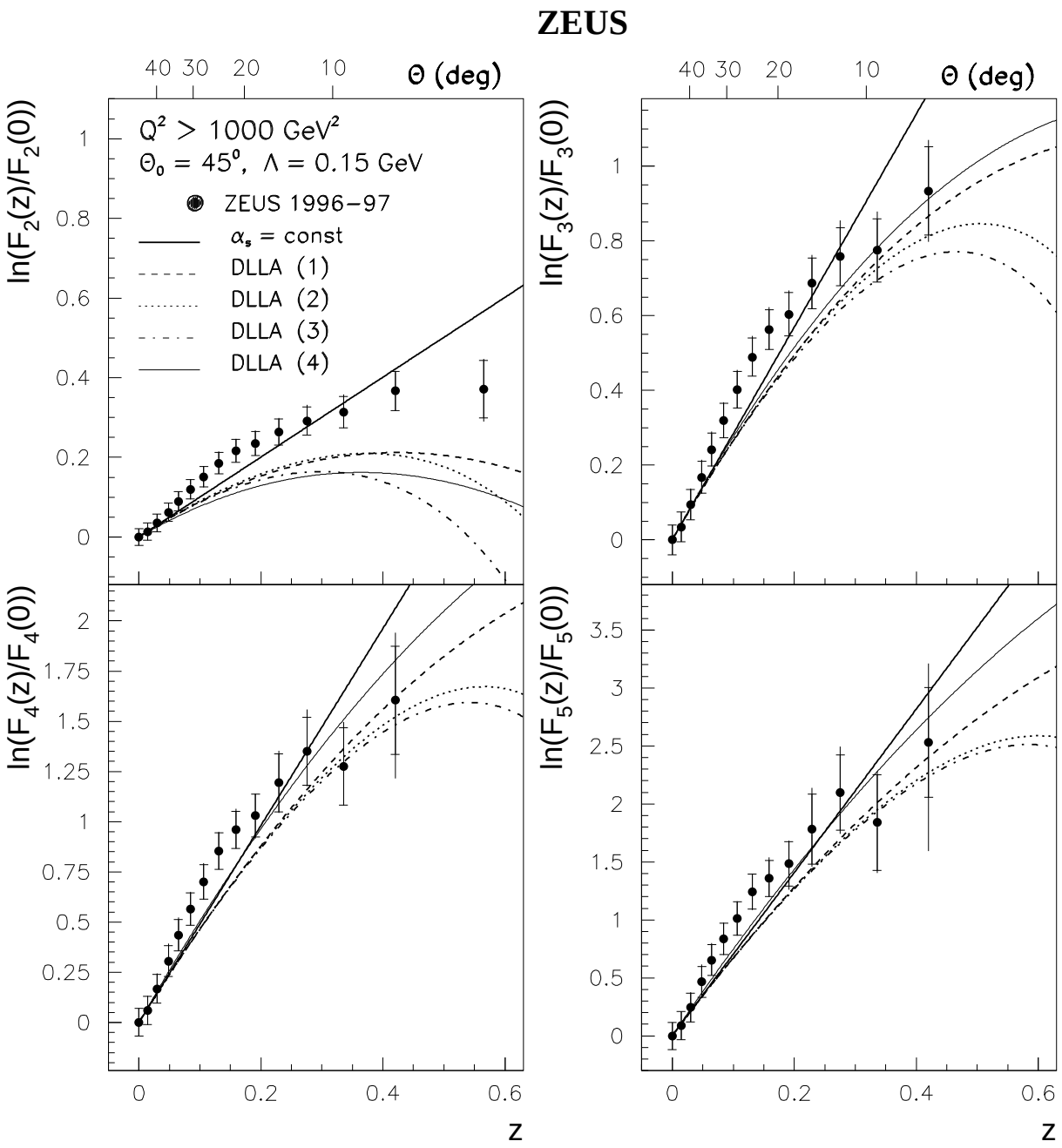

Figure 4: $F_q(z)/F_q(0)$ ($q = 2, \ldots, 5$) as a function of the scaling variable z for $\Theta_0 = 45^o$ and $\Lambda = 0.15$ GeV, compared to the QCD prediction of Eq. (2) with different parameterisations of D_q: $\alpha_s = const$ of Eq. (4) (bold solid lines); (1) DLLA of Eq. (5) (dashed lines); (2) DLLA of Eq. (6) (dotted lines); (3) DLLA of Eq. (7) (dash-dotted lines); and (4) DLLA with a correction from the MLLA [12] (thin solid lines). The values of Θ are given at the top of the plots. The inner error bars are statistical uncertainties; the outer are statistical and systematic uncertainties added in quadrature.

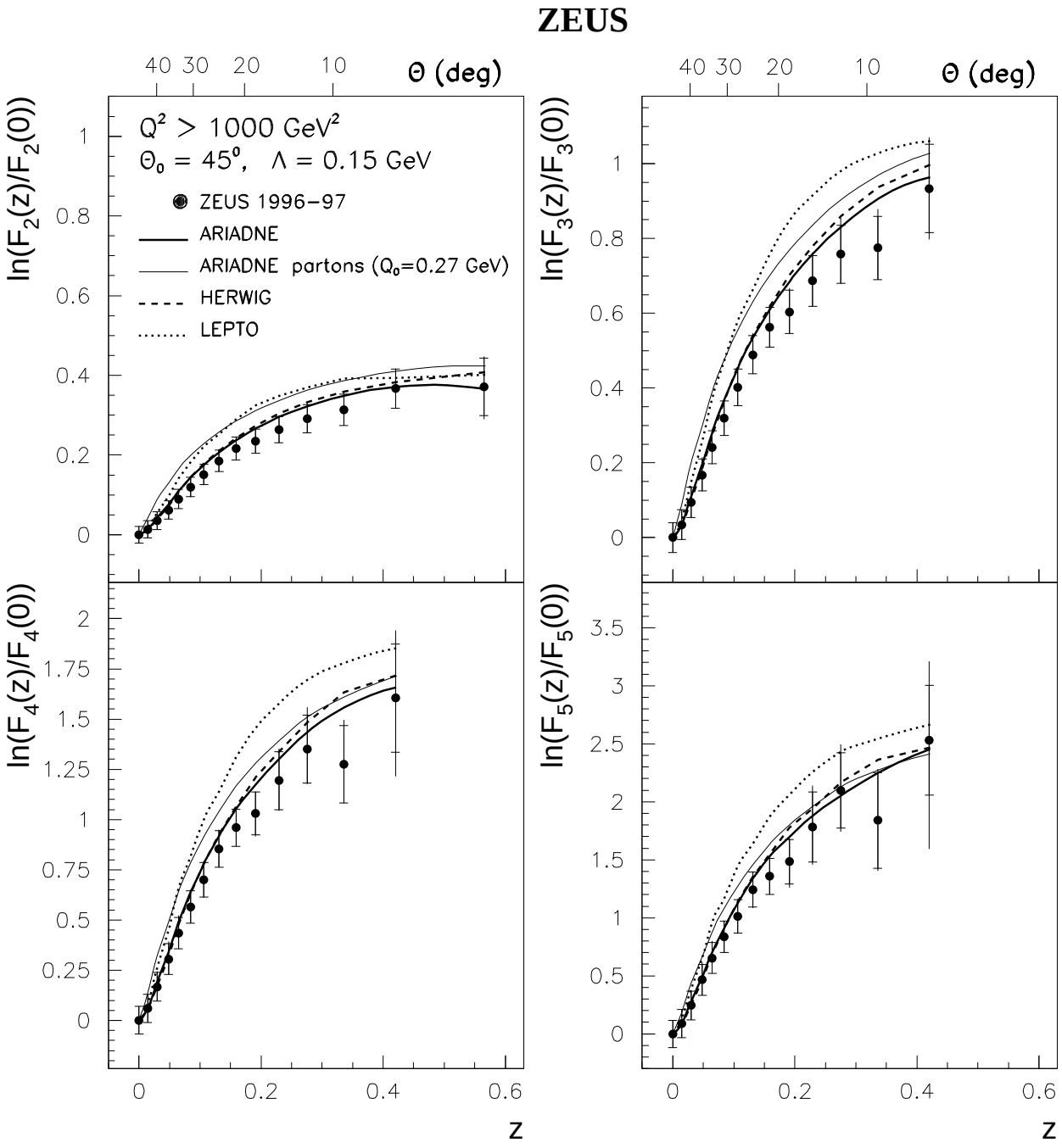

Figure 5: The data of Fig. 4 compared to different Monte Carlo models at the hadron level: ARIADNE (bold solid lines), HERWIG (bold dashed lines) and LEPTO (bold dotted lines). The thin solid lines show the parton-level prediction of ARIADNE with $Q_0 = 0.27$ GeV.